In Situ Study of Silver Electrodeposition at $MoSe_2$ by Electrochemical Scanning Tunneling Microscopy

Takashi Ohmori,[†,‡] Raúl J. Castro,[§] and Carlos R. Cabrera*[,†]

Department of Chemistry and Materials Research Center, University of Puerto Rico, Río Piedras Campus, P.O. Box 23346, San Juan, Puerto Rico 00931-3346, and Department of Chemistry, Cayey University College, University of Puerto Rico, Cayey, Puerto Rico 00736

Received April 9, 1998. In Final Form: September 9, 1998

The electrodeposition of Ag at $MoSe_2$ has been investigated, in situ, by electrochemical scanning tunneling microscopy (EC-STM). The process was investigated by observing $MoSe_2$ at fixed electrode potentials which were referenced to the onset potential in the cyclic voltammograms of Ag electrodeposition at $MoSe_2$. When an electrode potential more negative than the onset potential was applied to $MoSe_2$, continuous Ag bulk deposition occurred. Consistently, the scanning tunneling microscopy (STM) image showed Ag deposits which exhibit a growth mode between island and layer growth. In the STM images taken near the onset potential, a small amount of Ag, presumably with sub-monolayer level coverage, was thought to be deposited. This initial deposition occurred so as to make the $MoSe_2$ surface smooth in the STM images. STM imaging was difficult in the electrode potential region positive of the onset potential because the applied bias voltage became small. However, the STM images acquired during Ag deposition after applying such an electrode potential exhibited a characteristic morphological change, from which we infer that those processes were related to the $MoSe_2$ reaction with Ag.

Introduction

Metal deposition on semiconductors has been intensively studied by vacuum deposition methods.[1−3] Recently, there has been an increasing interest in the (photo)electrochemical deposition of metals at semiconductors with the purpose of creating Schottky or p−n junctions[4,5] or developing solar energy systems. It is known that various metals deposited on TiO_2[6] or Si[7−9] increase the efficiency of photoelectrochemical cells. The electrochemical deposition of transition metals on semiconductors has been studied by Memming[1] and others.[2,3]

In previous publications, we have presented studies on the (photo)electrodeposition processes of Ag[10] and Cu[11] on $MoSe_2$. It was clarified that, for Ag deposition, deposited Ag reacted with $MoSe_2$, while, for Cu deposition, intercalation of Cu occurred into the $MoSe_2$. Focusing on Ag deposition, we had concluded that $MoSe_2$ reacts with Ag via a displacement reaction which produces Ag_2Se and MoO_3. From the cyclic voltammograms (CVs), which exhibited qualitatively the same behavior with and without illumination, it was found that $MoSe_2$ reacted with Ag irrespective of the presence of illumination. The reaction occurred simply by cycling the $MoSe_2$ electrode potential in the electrolyte solution containing Ag^+ ion. Therefore, to understand the Ag deposition process on $MoSe_2$, including the reaction of Ag with $MoSe_2$, it is important to observe how the morphology of $MoSe_2$ changes with the electrode potential.

Scanning probe microscopy techniques such as scanning tunneling microscopy (STM) or atomic force microscopy (AFM) have been used extensively to study in situ electrodeposition processes on metal electrodes.[12] In contrast, few investigations have been reported on this process at semiconductor electrodes.[13−16] Among them, Thundat et al. studied the deposition of Ni on Ge by STM to find that the deposition mode changes from layer to island growth at a few layers coverage.[13] Uosaki and coworkers investigated Cu on GaAs by AFM to show that the way in which the deposition proceeds depends on the initial GaAs structure.[14] They also reported STM observations of Sn deposition on GaAs.[15] Yoshihara et al. showed in a STM study of Pt on p-Si that crystal growth predominates over nucleation in the dark, while under illumination nucleation predominates.[16] To better understand the electrodeposition process, there is a need to study how the reaction takes place in the entire electrode potential region comprising the electrodeposition, that is, in regions both positive and negative of the onset potential

* To whom correspondence should be addressed. E-mail: cabrera@web.uprr.pr.

† Department of Chemistry and Materials Research Center, University of Puerto Rico.

‡ Present address: Research Institute of Innovative Technology for the Earth (RITE), 9-2, Kizugawadai, Kizu-cho, Soraku-gun, Kyoto 619-0292, Japan.

§ Department of Chemistry, Cayey University College, University of Puerto Rico.

(1) Reineke, R.; Memming, R. *Surf. Sci.* **1987**, *192*, 66.

(2) Allongue, P. In *Physics and Applications of Semiconductor Electrodes Covered with Metal Clusters*; Conway, B. E., Bockris, J. O'M., White, R. E., Eds.; Modern Aspects of Electrochemistry Series; Plenum Press: New York, 1992; Vol. 23, Chapter 4.

(3) Schlesinger, R.; Rogaschewski, S.; Janietz, P. J. *Phys. Status Solidi A* **1990**, *120*, 687.

(4) Allongue, P.; Souteyrand, E.; Allemand, L. *J. Electrochem. Soc.* **1989**, *136*, 1027.

(5) Allongue, P.; Souteyrand, E. *J. Vac. Sci. Technol.* **1987**, *B5*, 1644.

(6) Bard, A. J. *J. Photochem.* **1979**, *10*, 59.

(7) Nakato, Y.; Tsubomura, H. *J. Photochem.* **1985**, *29*, 257.

(8) Hinogami, R.; Mori, T.; Yae, S.; Nakato, Y. *Chem. Lett.* **1994**, 1725.

(9) Hinogami, R.; Nakamura, Y.; Yae, S.; Nakato, Y. *Appl. Surf. Sci.* **1997**, *121*, 301.

(10) Castro, R. J.; Cabrera, C. R. *Langmuir* **1995**, *11*, 1375.

(11) Castro, R. J.; Cabrera, C. R. *J. Electrochem. Soc.* **1992**, *139*, 3385.

(12) *Nanoscale Probes of the Solid/Liquid Interface*; Gewirth, A. A., Siegenthaler, H., Eds.; NATO-ASI Series 288; Kluwer Academic Publishers: Dordrecht, 1995.

(13) Thundat, T.; Nagahara, L. A.; Lindsay, S. M. *J. Vac. Sci. Technol.* **1990**, *A8*, 539.

(14) Koinuma, M.; Uosaki, K. *Electrochim. Acta* **1995**, *40*, 1345.

(15) Eriksson, S.; Carlsson, P.; Holmstrom, B.; Uosaki, K. *J. Electoanal. Chem.* **1992**, *336*, 217.

(16) Yoshihara, S.; Endo, K.; Sato, E.; Bockris, J. O'M. *J. Electroanal. Chem.* **1994**, *372*, 91.

10.1021/la980405l CCC: $15.00
Published on Web 10/21/1998

of the reaction. In electrochemical scanning tunneling microscopy (EC-STM) studies, such features (e.g., the surface structure comprising adsorbate and substrate and its changes with electrode potential) have been intensively investigated for metal electrodes.[12] In contrast, few papers have dealt with such aspects for semiconductor electrodes. This is partly because changing the electrode potential of the semiconductor affects the STM imaging conditions, resulting in a limitation on the range of electrode potentials which can be studied by EC-STM. Recently, we have been investigating such processes on $MoSe_2$ electrodes by in situ EC-STM.[17,18] In the present paper, we have attempted to address the subject mentioned above. That is, we studied, in situ, Ag electrodeposition on $MoSe_2$ without illumination using EC−STM. In this work, we observed $MoSe_2$ surfaces at fixed electrode potentials, referenced to the onset potential of Ag electrodeposition at $MoSe_2$.

Experimental Section

The p-$MoSe_2$ samples used in this work were the same as those described in our previous papers.[10,11] Briefly, p-$MoSe_2$ was synthesized by chemical vapor transport with Se as a transporting agent. Cyclic voltammetry was measured using a Princeton Applied Research (PAR) 173 potentiostat, a PAR universal programmer 175, and a Soltec VP-64243 x−y recorder. The scanning tunneling microscopy (STM) observations were performed with a Digital Instruments (DI) Nanoscope IIIa. The images were acquired with a tunneling current of 1 nA and scanning frequencies between 1 and 3 Hz in the *x* and between 0.004 and 0.01 Hz in the *y* direction. All the STM images presented herein were flattened using DI's first-order line fit. The electrochemical STM cell consisted of Pt wire quasi-reference and counter electrodes and the p-$MoSe_2$ working electrode. The Pt/Ir STM tips were purchased from DI and coated with Apiezon wax before being used in our experiments. The wax coating was applied simply by dipping the STM tips in a pot of melted Apiezon wax. The leakage current of each tip was monitored before and after the STM measurements in order to ensure the reliability of the STM images. The electrolyte solution used in the present experiments contained 0.25 M KNO_3 and 5 mM $AgNO_3$, which was the same solution used for our previous studies published elsewhere.[10] For comparison purposes, some STM images were taken in 0.25 M KNO_3, that is, in only the supporting electrolyte solution. The solutions used here were prepared from reagent grade chemicals and pure water (having 18 MΩ·cm conductivity) obtained from a Barnstead Nanopure system. All the electrode potentials presented here are with respect to a saturated calomel electrode (SCE). The electrode potential difference between the Pt quasi-reference and SCE reference electrodes was examined by comparing identical CVs which were acquired using both reference electrodes with the aforementioned electrochemical setup. Typically, the Pt quasi-reference electrode had an electrode potential positive of that of the SCE by 0.50 V in 0.25 M KNO_3 with 5 mM $AgNO_3$ and by 0.35 V for the solution of 0.25 M KNO_3.

Auger electron spectroscopy (AES) measurements were carried out using a PHI 660 scanning Auger microprobe. For the $MoSe_2$ AES analyses the $MoSe_2$ surface was removed from the EC−STM cell and cleaned thoroughly with pure water before placing it in the UHV system.

Results and Discussion

In electrochemical scanning tunneling microscopy experiments it is necessary to electrochemically characterize the STM tip and the substrate of interest. This is done to determine the potential that can be applied to the STM tip and, in our case, the $MoSe_2$ substrate. In Figure 1 we present the respective cyclic voltammograms (CVs) of an $MoSe_2$ sample and a Pt/Ir STM tip, both obtained in 0.25 M KNO_3 containing 5 mM $AgNO_3$. It is found in Figure 1a that the cathodic current for Ag deposition on the $MoSe_2$ starts to flow at approximately 0.5 V versus SCE. The cyclic voltammetry behavior of the $MoSe_2$ varied somewhat from sample to sample. Probably, this depends partly on the density of axial planes exposed at the $MoSe_2$ surface. The degree of exposed axial planes as well as surface cleanliness was always checked microscopically before performing each experiment by observing the surface with an optical microscope. The CV is supposed to depend also on lattice defects in the $MoSe_2$ such as atomic vacancies[19] or excess selenium.[20] We confirmed the existence of atomic vacancies in our $MoSe_2$ sample by imaging the surface with atomic scale STM magnifications in air.

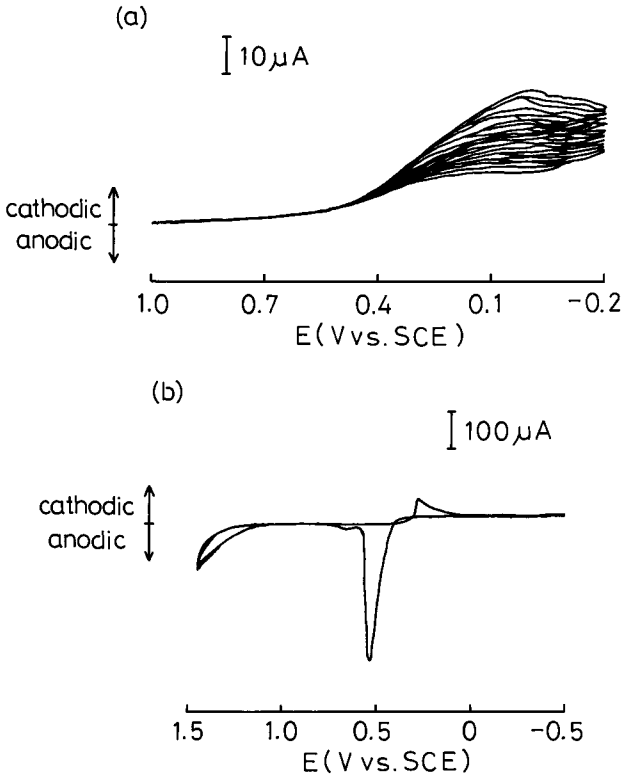

Figure 1. Cyclic voltammograms of (a) $MoSe_2$ and (b) a Pt/Ir STM tip in 0.25 M KNO_3 with 5 mM $AgNO_3$. The sweep rate was 20 mV/s for part a and 50 mV/s for part b. The CV in part a was acquired after the anodic stripping current disappeared.

It was frequently observed that the anodic current for Ag stripping flowed in the first few cycles, after which the anodic current decreased gradually and disappeared. On the other hand, typically the cathodic current for Ag deposition increased with cycling. These experimental facts are considered to be evidence suggesting that Ag physically deposited on the $MoSe_2$ surface or Ag deposited on Ag can be stripped off by potential cycling while the Ag reacted with $MoSe_2$ cannot.

In the CV of the Pt/Ir STM tip (Figure 1b), it is seen that Ag deposition and desorption occur at approximately 0.3 and 0.55 V versus SCE, respectively, and that surface oxidation starts from approximately 1.1 V versus SCE. From this CV, the electrode potential which can be applied to the STM tip for in situ STM imaging[17] is found to be between 0.55 and 1.1 V versus SCE.

Prior to describing the results, it should be noted that the electrode potential applied to the $MoSe_2$ has two roles: one is as the potential at which Ag deposition

(17) Ohmori, T.; Cabrera, C. R. *Langmuir* **1998**, *14*, 3723.
(18) Ohmori, T.; Castro, R. J.; Cabrera, C. R. *Langmuir*, in press.
(19) Cincotti, S.; Rabe, J. P. *Appl. Phys. Lett.* **1993**, *62*, 3531.
(20) Bindra, P.; Gerischer, H.; Kolb, D. M. *J. Electrochem. Soc.* **1977**, *124*, 1012.

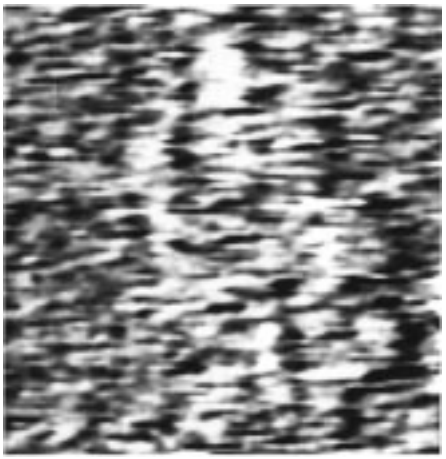

Figure 2. In situ STM image displaying the surface morphology of an Ag deposit on $MoSe_2$ observed at 0 V versus SCE in 0.25 M KNO_3 with 5 mM $AgNO_3$. The STM tip potential was 1.0 V versus SCE. The scan size was 200 nm × 200 nm, and the black to white vertical height scale covers 3.5 nm. White features are tallest, and black features are shortest. Figure 3b presents a picture of the surface in an inert solution (0.25 M KNO_3) under similar imaging conditions.

processes are studied, and the other is as an STM imaging condition. As an STM imaging condition, the electrode potential determines the bias voltage and band bending of the semiconductor $MoSe_2$. Band bending also affects the Ag deposition process. First, we investigated electrode potentials negative of the onset potential of Ag deposition. Figure 2 was acquired with the electrode potential of the $MoSe_2$ fixed at 0 V versus SCE. In this case, the cathodic current continued to flow and the $MoSe_2$ surface exhibited successively occurring Ag deposition. In Figure 2, we see randomly deposited Ag with some amorphous hillocks on the $MoSe_2$ surface. Because bulk deposition is regarded as a system where the deposit and substrate are the same (in the present case, Ag on Ag), the growth mode which was observed in Figure 2, that is, intermediate between layer and island growth, will be expected.[20] The observed uniformity of the Ag deposit may be in part caused by the effect of the STM tip scanning. That is, the tip scanning seemed to prevent Ag deposition onto the scanning area and also seemed to move the Ag deposits along the $MoSe_2$ surface. Further, the STM imaging of Ag deposition was frequently prevented by an increase in the leakage current of the STM tip. This was probably because Ag deposition proceeded abruptly at certain locations in the vicinity of the scanning area, causing the contact of the Ag deposit with the STM tip. The deposited Ag was stripped off instantly from the $MoSe_2$ surface when the electrode potential was swept in the positive direction.

Next, we measured the $MoSe_2$ surface with the electrode potential fixed at +0.5 V versus SCE, that is, a potential nearly equal to the onset potential for Ag deposition. Figure 3a shows an STM image of the $MoSe_2$ observed in 0.25 M KNO_3 with 5 mM $AgNO_3$. For comparison, we also present in Figures 3b and 3c STM images obtained in 0.25 M KNO_3, that is, in only the supporting electrolyte. The images were observed at 0 V versus SCE for Figure 3b and 0.5 V versus SCE for Figure 3c, respectively. In 0.25 M KNO_3, it is seen that the $MoSe_2$ shows a very flat surface at 0 V versus SCE. This topography was stable throughout the time required for STM measurements, for example, typically approximately 30 min. At 0.5 V versus SCE, the $MoSe_2$ surface was not stable and changed with time due to oxidation of the surface, that is, surface etching.[18] It is found in Figure 3c that many pits have been nucleated on

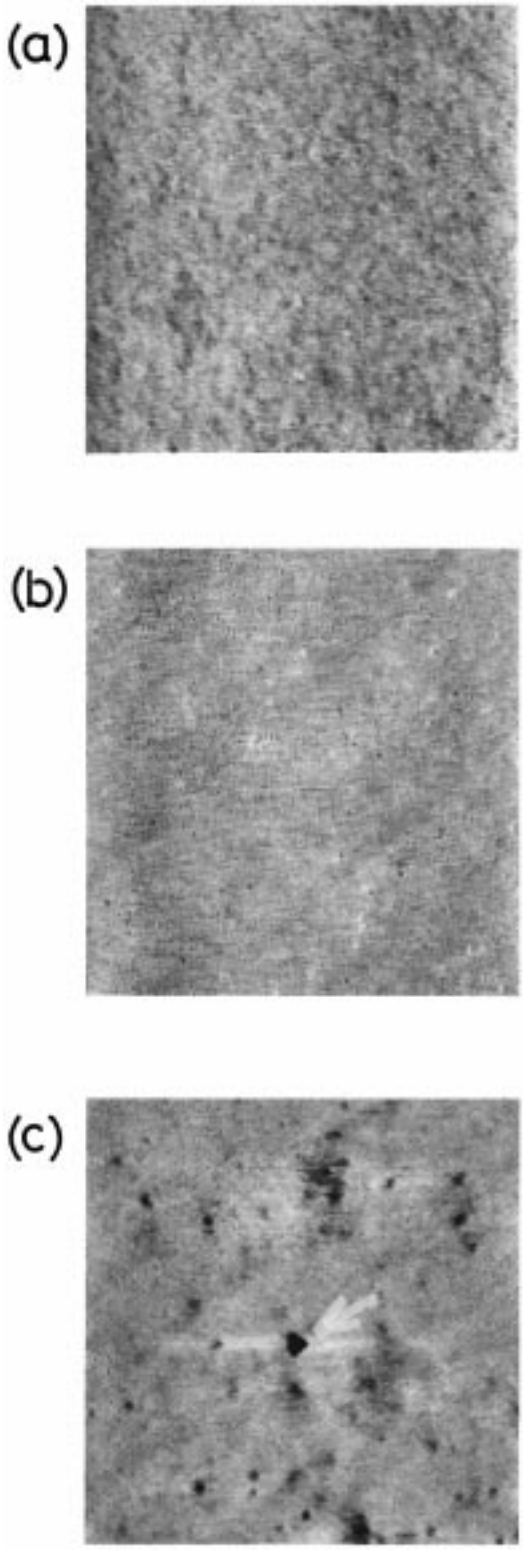

Figure 3. In situ STM images of the $MoSe_2$. The imaging conditions [the electrode potential of the $MoSe_2$ sample (E_s versus SCE), the STM tip potential (E_t versus SCE), and the electrolyte solution used] were as follows: (a) $E_s = 0.5$ V and $E_t = 1.05$ V in 0.25 M KNO_3 with $AgNO_3$; (b) $E_s = 0$ V and $E_t = 0.9$ V in 0.25 M KNO_3; (c) $E_s = 0.5$ V and $E_t = 0.9$ V in 0.25 M KNO_3. The scan sizes were 500 nm × 500 nm, and the black to white color height scales cover 3.5 nm for all images.

the basal plane of the $MoSe_2$. Moreover, a pit which has grown to possess a triangular shape is also seen (arrowed).[18] On the other hand, we can see in Figure 3a a different morphology from that in Figure 3c. That is, the

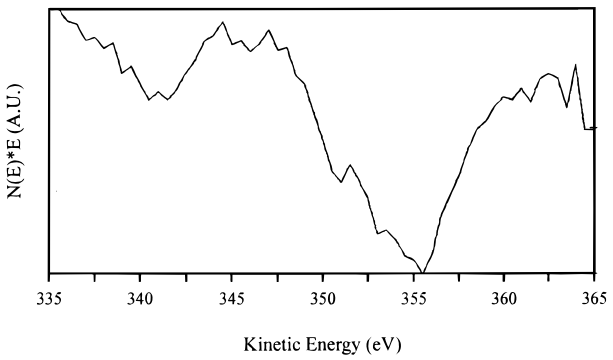

Figure 4. AES spectrum in the vicinity of the Ag(MNN) Auger line for an $MoSe_2$ electrode held at an electrode potential of 0.5 V versus SCE for 10 min in a solution of 0.25 M KNO_3 and 5 mM $AgNO_3$. The Ag Auger (MNN) peaks ocurring at 351 and 356 eV are indicative of a Ag surface concentration below 1%.

pits observed in Figure 3c cannot be recognized in Figure 3a. In addition, the surface is found to be smoother compared to that for Figure 3c. This morphological difference between parts a and c of Figure 3 would reasonably imply that some amount of Ag has been deposited on the $MoSe_2$ surface in Figure 3a, even at a potential approximately equal to the onset potential for Ag electrodeposition. Actually, the existence of Ag was confirmed by AES measurements of this surface (Figure 4). There are AES electron kinetic energy signals at 351 and 356 eV for the Ag(MNN) Auger transition, indicating the presence of Ag on the surface. Its surface concentration is below 1%. At this applied potential, oxidation of the $MoSe_2$ surface and Ag deposition were occurring simultaneously; where pits were formed by the oxidation reaction, they were filled with Ag deposits. Another way of seeing this is that the oxidation reaction at the surface was restrained by the Ag deposition event onto the sites where oxidation would otherwise have been most readily initiated. In either case, only a small amount of Ag, with sub-monolayer coverage, is presumed to be deposited. During this experiment we observed a distinct current at this applied potential, not seen in either the cathodic direction, originating from Ag deposition, or the anodic direction, caused by the oxidation reaction, as is shown in the CV of Figure 1a.

To further investigate this initial Ag deposition process, we observed the $MoSe_2$ successively first at 0.8 V versus SCE and then at 0.2 V versus SCE. Figure 5a shows an STM image of the $MoSe_2$ surface which was obtained by first fixing the electrode potential at 0.8 V versus SCE. Here we see a rougher surface compared to that in Figure 3a. This is reasonable because oxidation of the surface is more pronounced at 0.8V versus SCE than at 0.5 V versus SCE, while Ag deposition is less rapid at 0.8 V versus SCE. Next, the electrode potential was swept to 0.2 V versus SCE and the STM image presented in Figure 5b was obtained. In this experiment we find that the surface became smooth compared to that in Figure 5a, which is a morphological change similar to that observed in going from Figure 3c to Figure 3a. A cathodic current passed for several minutes after the electrode potential was changed to 0.2 V versus SCE; then it gradually decreased, approaching no current. This indicates that a certain amount of Ag deposition took place and then the deposition ceased. These STM images of Figure 5 support the idea that Ag deposition was taking place in Figure 3a and show, directly, that Ag deposition in the initial stage proceeds so as to make the $MoSe_2$ surface smooth. It might be possible to attribute this morphological change (from a rough to a smooth surface) to a reduction in STM imaging

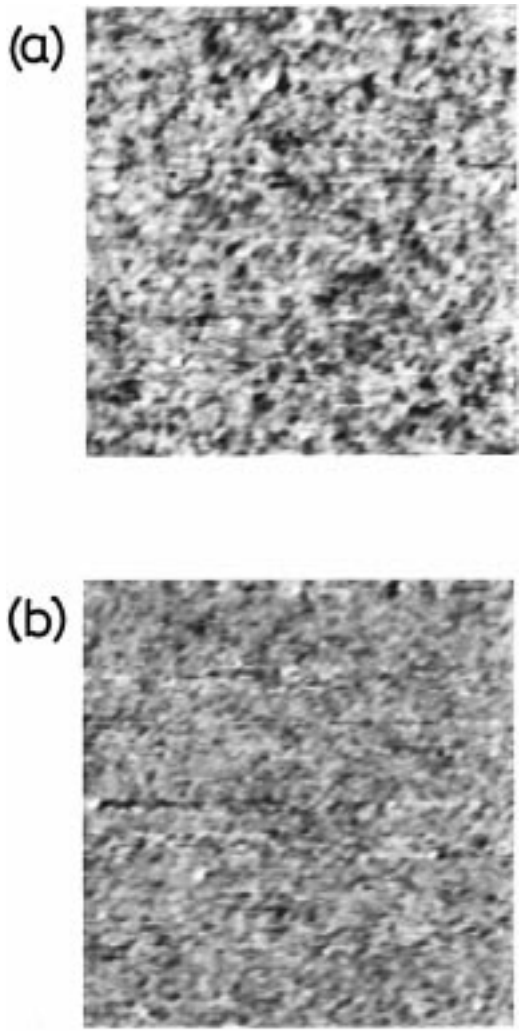

Figure 5. In situ STM images of $MoSe_2$ observed (a) at 0.8 V versus SCE and (b) at 0.2 V versus SCE in 0.25 M KNO_3 with 5 mM $AgNO_3$. The STM imaging conditions were as follows for both the images: 1.05 V versus SCE STM tip potential, 252 nm × 252 nm scan size, and 3.5 nm height scale.

resolution resulting from blunting or contamination of the STM tip. However, this possibility can be excluded because we could, upon changing the $MoSe_2$ electrode potential, again observe STM images which exhibited the change from a smooth to a rough surface.

Because an ideal (i.e. defect-free) basal plane does not have any electronic states within the band gap, we can consider two different sites on the $MoSe_2$ surface where this initial Ag deposition occurs: one is at step sites, and the other is at lattice defects such as atomic vacancies or excess selenium atoms which are exposed on the $MoSe_2$ surface. Lattice defects can have impurity levels (i.e. surface states) within the band gap of the $MoSe_2$.[17] When the electrode potential is raised enough to fill these levels, such defect sites will be favorable for Ag deposition and reduction to occur. The valence and conduction band edges and the Fermi level of the $MoSe_2$ used here are located at 0.9, − 0.5, and 0.8 V versus SCE, respectively.[11,21] Thus, the electrode potentials which were applied in Figures 3a (+0.5 V versus SCE) and 5b (0.2 V versus SCE) possibly meet this condition. On one hand, bulk deposition will be prohibited until the electrode potential is raised further,

(21) Castro, R. J. Ph.D. Thesis, University of Puerto Rico, July 1996.

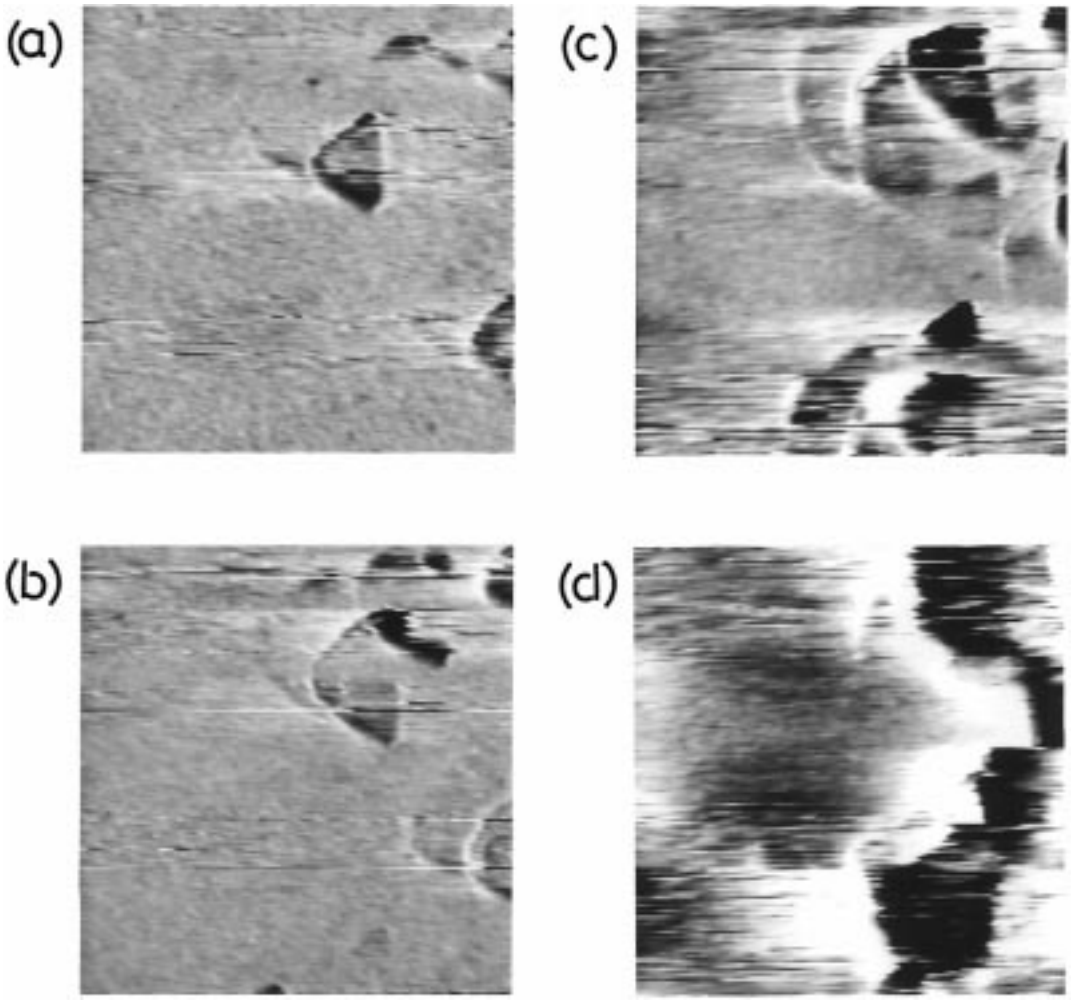

Figure 6. Sequential in situ STM images of the $MoSe_2$ observed at 0 V versus SCE in 0.25 M KNO_3 with 5 mM $AgNO_3$ after applying an electrode potential of 1.3 V versus SCE for 15 min: (a) immediately following the change to 0 V versus SCE; (b) 3 min later; (c) 7 min later; (d) 9 min later. The STM imaging conditions for all the images were as follows: 1.05 V versus SCE STM tip potential, 500 nm × 500 nm scan size, and 40 nm height scale.

providing enough electron density[22] at the $MoSe_2$ surface (compare the case in Figure 2). Ag bulk deposition by hole injection is not thought to occur either, because the redox potential of Ag^+/Ag (0.56 V versus SCE[23]) is located within the band gap of the $MoSe_2$.[20] The smoothing of the surface by Ag deposition would be possible if we consider that STM images represent not only geometrical but also electronic structures of the surface.[24−26] As step sites, which exist naturally or are created by oxidation reactions, have dangling bonds which are able to provide surface states within the band gap, the Ag deposition (reduction reaction) will occur at such sites in the same way it does at lattice defects. In such a case, the surface smoothing could be interpreted as an indication that geometry dominates the STM current in this case.

To study the effect of potential application in the more positive region of the Ag deposition, STM measurements were performed after cycling the electrode potential 15 times between 1.0 and − 0.2 V versus SCE. However, noticeable morphological changes could not be observed. Additionally, the $MoSe_2$ surface could not be imaged stably at relatively positive electrode potentials (at 1.0 V versus SCE) because the bias voltage became too small. In light of these problems, we performed the following experiment in order to investigate the effect in a distinct manner. The electrode potential of the $MoSe_2$ was first fixed at +1.3 V versus SCE for 15 min without imaging and then changed to 0 V versus SCE so that we could observe the Ag deposition process. Figure 6 shows time-sequential STM images taken after the electrode potential was changed to 0 V versus SCE. It is seen that the initial etched areas (Figure 6a), which were formed by the potential application of 1.3 V versus SCE, deformed (Figure 6b and c) and that, finally, large hillocks were formed (Figure 6d) by Ag deposition. When the electrode potential for Ag deposition (0 V versus SCE) was applied immediately (Figure 2), that is, without prepolarization, we did not see a morphological transformation such as that observed in Figure 6. Neither did we recognize it in the identical experiment performed in 0.25 M KNO_3 only. In KNO_3, in the absence of Ag ion, we observed a flat surface and occasionally an etched area formed by the prepolarization. The etched area did not change its morphology during the STM measurement, in contrast to what was observed in Figure 6. Consequently, we propose that the reaction

(22) Sze, S. M. *Physics of Semiconductor Devices*; John Wiley & Sons: New York, 1969.
(23) *CRC Handbook of Chemistry and Physics*, 71st ed.; CRC Press: Boca Raton, FL, 1990; p 8-16.
(24) Giancarlo, L.; Cyr, D.; Muyskens, K.; Flynn, G. W. *Langmuir* **1998**, *14*, 1465.
(25) Venkataraman, B.; Flynn, G. W.; Wilbur, J. L.; Folkers, J. P.; Whitesides, G. M. *J. Phys. Chem.* **1995**, *99*, 8684.
(26) Claypool, C. L.; Faglioni, F.; Goddard, W. A.; Gray, H. B.; Lewis, N. S.; Marcus, R. A. *J. Phys. Chem.* **1997**, *101*, 5978.

$$MoSe_2 + 4Ag^+ + 3H_2O \rightarrow 2Ag_2Se + MoO_3 + 4H^+ + H_2 \quad (6)$$

occurred in addition to the $MoSe_2$ oxidation reaction during the 1.3 V versus SCE prepolarization of the surface shown in Figure 6a. The reacting Ag^+ ion is thought to be supplied from the electrolyte solution. The Ag ion will be able to reach the $MoSe_2$ surface without being reduced, different from the case in Figures 3a or Figure 5b, because the electrode potential of +1.3 V versus SCE is positive of the redox potential of Ag^+/Ag. The STM images in Figure 6 clearly show that the process is not simple physical Ag deposition onto the surface. The possible processes leading to this morphological change would be Ag deposition and diffusion from the outermost to the inner surface, the above reaction, structural relaxation of Ag_2Se, dissolution of MoO_3,[10,27] or a combination of these processes which may be induced by Ag deposition. The experimental fact seen in the CV, that Ag stripping was observed in only the first few cycles, after which it decreased and disappeared, seems to suggest that once an Ag_2Se layer is formed on the surface, further deposited Ag becomes easily incorporated without being stripped off. This would be consistent with the above inference that Ag_2Se was formed when a potential of 1.3 V versus SCE was applied to the electrode, followed by the deposition of Ag at 0 V versus SCE, causing the observed characteristic morphological change. We believe that when the electrode potential of the $MoSe_2$ is cycled,[10] Ag reacts to form Ag_2Se in the positive electrode potential region and that more Ag_2Se is grown as more Ag is deposited in the negative potential region. We should note that the morphological change (especially that seen in going from Figure 6a to Figure 6c) is reminiscent of the reaction process of surface etching.[18] Clarifying the relationship between the reaction of $MoSe_2$ with Ag and the oxidation of $MoSe_2$ is an important problem to be solved. It is plausible that the oxidation reaction helps the former reaction take place and proceed deeper into the surface[10] by etching the $MoSe_2$ and providing reactive step sites. Further detailed analyses on changes in surface composition with morphology will have to be done in order to obtain more insight into the reaction process of Ag with $MoSe_2$.

In summary, we have studied Ag electrodeposition on $MoSe_2$, in situ, using EC−STM. The $MoSe_2$ surface was observed at fixed electrode potentials referenced to the onset potential of Ag deposition on $MoSe_2$. Bulk-deposited Ag was recognized at an electrode potential negative of the onset potential while a sub-monolayer amount of Ag was presumed to be deposited around the onset potential, which made the $MoSe_2$ surface smooth in the STM images. The STM images observed during Ag deposition on a $MoSe_2$ surface exposed to an electrode potential positive of the onset potential exhibited a characteristic morphological change, from which we inferred that these processes were related to the reaction of $MoSe_2$ with Ag.

Acknowledgment. The authors acknowledge the financial support of NSF-EPSCoR grant number OSR-9452893 and DOD-EPSCoR grant number P-35825-CH-DPS. We would like to thank one of the reviewers for very helpful comments and for helping with the editing of the final version of the manuscript.

LA980405L

(27) Bohmisch, M.; Burmeister, F.; Boneberg, J.; Leiderer, P. *Appl. Phys. Lett.* **1996**, *69*, 1882.